Functionalization of Industrial Polypropylene Films via the Swift-Heavy-Ion-Induced Grafting of Glycidyl Methacrylate

S. Chawla,[1] A. K. Ghosh,[2] D. K. Avasthi,[3] P. Kulriya,[3] S. Ahmad[4]

[1]*Amity School of Engineering and Technology, New Delhi, India*
[2]*Centre for Polymer Science and Engineering, Indian Institute of Technology, New Delhi, India*
[3]*Inter-University Accelerator Center, Aruna Asaf Ali Marg, New Delhi, India*
[4]*Materials Research Laboratory, Department of Chemistry, Faculty of Natural Science, Jamia Millia Islamia, New Delhi 110025, India*

Received 12 October 2006; accepted 15 January 2007
DOI 10.1002/app.26425
Published online 5 June 2007 in Wiley InterScience (www.interscience.wiley.com).

ABSTRACT: Swift-silver-ion irradiation was explored as a means of forming chemically active sites on the surface of biaxially oriented polypropylene films. The active species, formed in air, was used to induce the graft copolymerization of glycidyl methacrylate in an aqueous solution. The surface structure, crystallinity, morphology, and hydrophilicity of the grafted samples were characterized with Fourier transform infrared, UV, wide-angle X-ray diffraction, scanning electron microscopy, and contact-angle measurements. Glycidyl methacrylate could be grafted onto biaxially oriented polypropylene after swift-heavy-ion irradiation without an additional initiator. The contact angle of the modified films decreased with the grafting percentage of glycidyl methacrylate on the polypropylene. The swift silver ions induced significant grafting only in small regions (i.e., the latent tracks) of the polymer. Furthermore, as the fluence of swift heavy ions increased beyond an optimum value, the overlapping of the latent tracks reduced the grafting yield. The observed findings could be very useful in developing an initiator-free grafting system. © 2007 Wiley Periodicals, Inc. J Appl Polym Sci 105: 3578–3587, 2007

Key words: films; graft copolymers; poly(propylene) (PP); structure-property relations

INTRODUCTION

Polypropylene (PP) possesses the most important volume share of the plastics industry because of its low cost, versatile properties, and growing commercial applications. However, PP is limited in its applications in several technologically important fields because of its lack of chemical functionalities, high sensitivity to photooxidation and/or thermal oxidation, low paintability, low dyeability, low elastic modulus, limited impact strength, poor adhesion to metal or glass, and poor compatibility with other polymers, including engineering plastics.[1] One of the most common methods used for the improvement of these disadvantages is to graft polar monomers onto the surface of PP.

Glycidyl methacrylate (GMA) is a bifunctional monomer containing an unsaturated group capable of free-radical grafting onto polyolefins (e.g., polyethylene and PP), together with a highly electrophilic epoxide moiety that can react with different nucleophilic functional groups such as carboxylic, hydroxide, and amine groups. As an epoxide moiety of GMA grafted onto a polyolefin is reacted with different nucleophilic reagents, it can be modified to alcohols,[2] amines,[3] phosphonic acid,[4] sulfonic acid,[5] and so on.

Grafting is a process by which chemical groups are attached by covalent bonds to a polymer backbone, usually via an aliphatic carbon atom. Grafting polymerization can be initiated by many methods, such as UV light, γ rays, plasma, and chemicals. However, there are still some limitations in the conventional grafting methods: plasma grafting is slow and expensive and has found only limited applications, γ rays can damage polymer structures over long-time exposures, UV light is harmful to human health, and the use of chemical initiators has resulted in the production of significant amounts of homopolymers. The undesired homopolymers not only waste expensive starting materials but also make processing more laborious.[6]

The grafting of GMA onto PP using conventional methods is a well-established phenomenon and has been extensively studied. Previously, Liu et al.[7] reported the grafting of GMA onto PP, using peroxide initiators, and they used the grafted PP in the reactive

Correspondence to: S. Ahmad (sharifahmad_jmi@yahoo.co.in).
Contract grant sponsor: Inter-University Accelerator Center (India).

compatibilization of PP blends with nitrile rubbers.[7] Sun et al.[8] studied the melt grafting of GMA onto PP in the presence of a comonomer, styrene, which improved the grafting yield and reduced the chain degradation of PP. They also reported the melt grafting of GMA onto PP in a twin-screw extruder.[9] Peseteskii and Makarenko[10] studied the efficiency of grafting of GMA to PP in an extruder and the degree of degradation of macromolecules in relation to the structure of the peroxide initiator. Pan et al.[11] first reported the modification of PP through the solid-phase grafting of GMA. Compared with other techniques, this method has many advantages, such as lower solvent requirements, a low temperature, low cost, and a low-pressure process, and the process also leads to a higher percentage of grafting.[12]

Swift heavy ions (SHIs) are heavy ions with kinetic energies of the order of 1 MeV per nucleon. They have the ability to deposit extremely high energy per unit of the ion path length. They are, therefore, characterized by extremely high linear energy transfer (LET) and are used for the nanometer-scale tailoring of surfaces in materials research.[13] When an SHI falls on a polymer film, it produces a damage zone around the incident path. The energy lost is spread, surrounding the path of the incident ion by the secondary electrons creating a cylindrical region with a high concentration of active sites. Therefore, a graft copolymer may be achieved when an active site in a polymer *X* initiates the polymerization of a monomer *Y*. In this way, inhomogeneous damage zones can be used to create special properties in the substrate polymer. SHI grafting is unique in the respect that it can generate surfaces with microdomains of modified and unmodified polymers. If the ion incidence is normal to the surface, then circular islands corresponding to the grafted domains are seen.[14] Moreover, in response to a stimulus, the grafted domains are transformed from an expanded conformation to a compact ball, leading to an increase or decrease in the pore size, and thus can be used for the production of permeability-adjustable membranes. These are also called intelligent membranes. Their potential applications include the controlled release of drugs.[15] Apparently, SHI can be used to bring about new properties not accessible with conventional chemical, radiochemical, or physical means.[16]

Efforts to synthesize graft copolymers using SHIs have been in progress since 1995.[17] The radiation grafting of acrylic acid, methyl methacrylate, and styrene onto PP foils irradiated with a 25-MeV proton beam was reported by Mazzei et al.[18] However, the attained knowledge about SHI-induced graft copolymerization is still much too limited, especially from an experimental point of view. This could be the first time that the active sites created by swift silver ions were used to initiate the graft copolymerization of GMA in PP. In this article, the structural changes in the grafted polymer are correlated with the changes in the crystallite size of PP. The purpose of this work is to study the SHI-induced grafting of GMA onto PP for its potential application as a compatibilizer in PP/Cloisite 30 B nanocomposites.

EXPERIMENTAL

Materials

Experiments were performed with commercially available biaxially oriented polypropylene (BOPP) films (15 μm thick) kindly supplied by Flex Industries, Ltd. (Noida, India). GMA, xylene, and acetone (analytical-reagent grade) were purchased from Aldrich (Steinheim, Germany) and used as received.

Synthesis of the graft copolymer

The BOPP film samples were irradiated in a vacuum at room temperature with a 15UD Pelletron accelerator at the Inter-University Accelerator Center (New Delhi, India). The 120-MeV Ag^{9+}-ion beams in the fluence range of 10^{10} to 3×10^{11} ions/cm^2 were used for irradiation. The ion-beam current was about 0.5–1 particle nA. The ion beam was scanned in an area of 10 mm × 10 mm with an electromagnetic scanner.

Before the irradiated BOPP film samples were used for grafting, they were stored at low temperatures (12 ± 3°C) in sealed plastic envelopes. The BOPP film samples were grafted with GMA with the peroxide method. In a typical grafting process, Ag^{9+}-ion-irradiated (120 MeV) BOPP was moistened with 0.04 mL of liquid GMA at room temperature for 24 h so that the GMA would be absorbed by the BOPP film. The GMA-moistened BOPP film was placed in a glass tube. To prevent the homopolymerization of GMA, an aqueous solution of 1 wt % Mohr's salt was also added. The glass tube was subsequently purged with nitrogen for 5 min and sealed. Afterwards, the glass tube was placed in an oven at 70°C for 50 h. The grafting was initiated by the thermal decomposition (70°C) of the peroxides in the presence of the monomer (GMA). After a given grafting period, the film was taken out from the glass tube, and the unreacted GMA monomer was extracted by the soaking and washing of the film in acetone and the drying of the film at room temperature in air to a constant mass. The GMA homopolymer adsorbed onto the film was washed off with a larger amount of acetone at 25°C for 24 h, and the film sample was dried at 70°C in a vacuum to a constant mass.

For the studies of the effects of the various parameters on the grafting polymerization, the grafting percentage (G_p) was determined according to the following equation:

$$G_p = [(W_g - W_0)/W_0] \times 100\% \quad (1)$$

where W_g and W_0 denote the weights of the grafted and ungrafted BOPP film samples, respectively.

Characterization

Fourier transform infrared (FTIR) spectra were recorded on a PerkinElmer FTIR RX1 (4000–500 cm^{-1}) spectrophotometer (Norwalk, CT) with a 4.0-cm^{-1} resolution.

The ultraviolet–visible (UV–vis) spectra were recorded on a PerkinElmer EZ-201 UV–vis spectrometer (400–190 nm) (Waltham, MA) with a 4-nm resolution.

Scanning electron microscopy (SEM) was performed by the observation of the surfaces of BOPP and grafted BOPP (PP-*g*-GMA) film samples under a scanning electron microscope (JSM-840, JEOL Co., Tokyo, Japan).

The contact angles of water droplets on the BOPP and PP-*g*-GMA surfaces were measured with a Rame-Hart model 100-00-230 goniometer (Netrong, NJ).

Wide-angle X-ray diffraction (WAXD) patterns were obtained with a Philips analytical X-ray PW1710 diffractometer (Almelo, The Netherlands) with the Cu Kα radiation at room temperature. The operating condition of the X-ray source was set at a voltage of 40 kV and a current of 30 mA in a range of $2\theta = 5$–35°. The scanning speed was 2.4°/min. The WAXD measurements were performed with a data acquisition time of 25 s per scan.

The crystallite size of PP was calculated according to the Scherrer equation:[19]

$$L = K\lambda/b\cos\theta \quad (2)$$

where L is the crystallite size (Å), b is the full width at half-maximum (fwhm; rad), λ is the wavelength of the X-ray beam (1.5425 Å), and K is a constant usually equal to 1.

RESULTS AND DISCUSSION

Mechanism of grafting

The swift silver ions (SHIs) abstract hydrogen atoms from PP during their passage through the BOPP film. This results in the formation of mainly surface radicals in polypropylene [PP*; eq. (3)]. When the PP radicals are in contact with air, they react with oxygen and lead to the formation of oxidized compounds such as peroxides and hydroperoxides [eq. (4)]. The peroxide and hydroperoxide groups on PP undergo a redox reaction with the ferrous ion of Mohr's salt [eq. (5)] to form an oxyl polymer radical (PPO*) capable of initiating graft copolymerization. Redox initiation usually results in mainly grafting polymerization with a minimum of homopolymerization because only PPO* is formed:[20]

$$PP + SHI \rightarrow PP^* \quad (3)$$

$$PP^* + O_2 \rightarrow PP\text{—}O\text{—}O\text{—}PP + PP\text{—}O\text{—}O\text{—}H \quad (4)$$

$$PP\text{—}O\text{—}O\text{—}PP + PP\text{—}O\text{—}OH + Fe^{2+} \rightarrow 3PP\text{—}O^* + OH^* + Fe^{3+} \quad (5)$$

On the basis of the experimental results, the following reaction mechanism is proposed.

The interaction of PPO* with the PP main chain is led by the abstraction of a hydrogen atom to either a tertiary radical [eq. (6)] or a secondary radical [eq. (7)]. The former can undergo a β-scission reaction. During the β-scission reaction, the main chain is broken into two parts, with a double bond on the one chain end and a secondary radical on the other chain end [eq. (8)]. The resulting degradation of the molecular weight is one limitation of the radical modification of PP in the molten state. This is the main reason for the development of radical reactions in the solid state.[21,22] Equations (6)–(18) in Scheme 1 describe some of the main reactions taking place during the grafting of GMA onto BOPP leading to the formation of GMA-grafted PP, that is, PP-*g*-GMA. However, some chain-transfer reactions in the propagation steps, eqs. (15)–(18), can lead to the formation of double bonds of dienes and trienes of PP chains. The growing chain radicals are mainly rooted on the film surface, and the grafting chains exist mostly in the form of a radical coil. Therefore, the growing chain radicals are not easily terminated by bimolecular reactions. The mobility of hydrogen radicals is far higher than that of growing chain radicals and oxyl macroradicals, so hydrogen radicals may move into the vicinity of a growing chain radical and terminate it [eq. (19)]. Disproportionation reactions can also lead to the termination of grafting polymerization [eq. (20)].

FTIR spectroscopy analysis

The FTIR spectrum of an unirradiated BOPP film is shown in Figure 1(a). It shows bands at 1328, 1304, 1256, 1168, 1103, 998, 940, 899, 841, and 809 cm^{-1}. These belong to the group of regularity bands, and they are related to different helix lengths of isotactic sequences.[23] However, the peaks at 973, 1377, and 1454 cm^{-1} represent segments residing predominantly in the amorphous region.[24] These bands and peaks indicate that the BOPP film was made from isotactic PP.

The variation of the electronic energy loss and nuclear energy loss of swift silver ions in PP with the

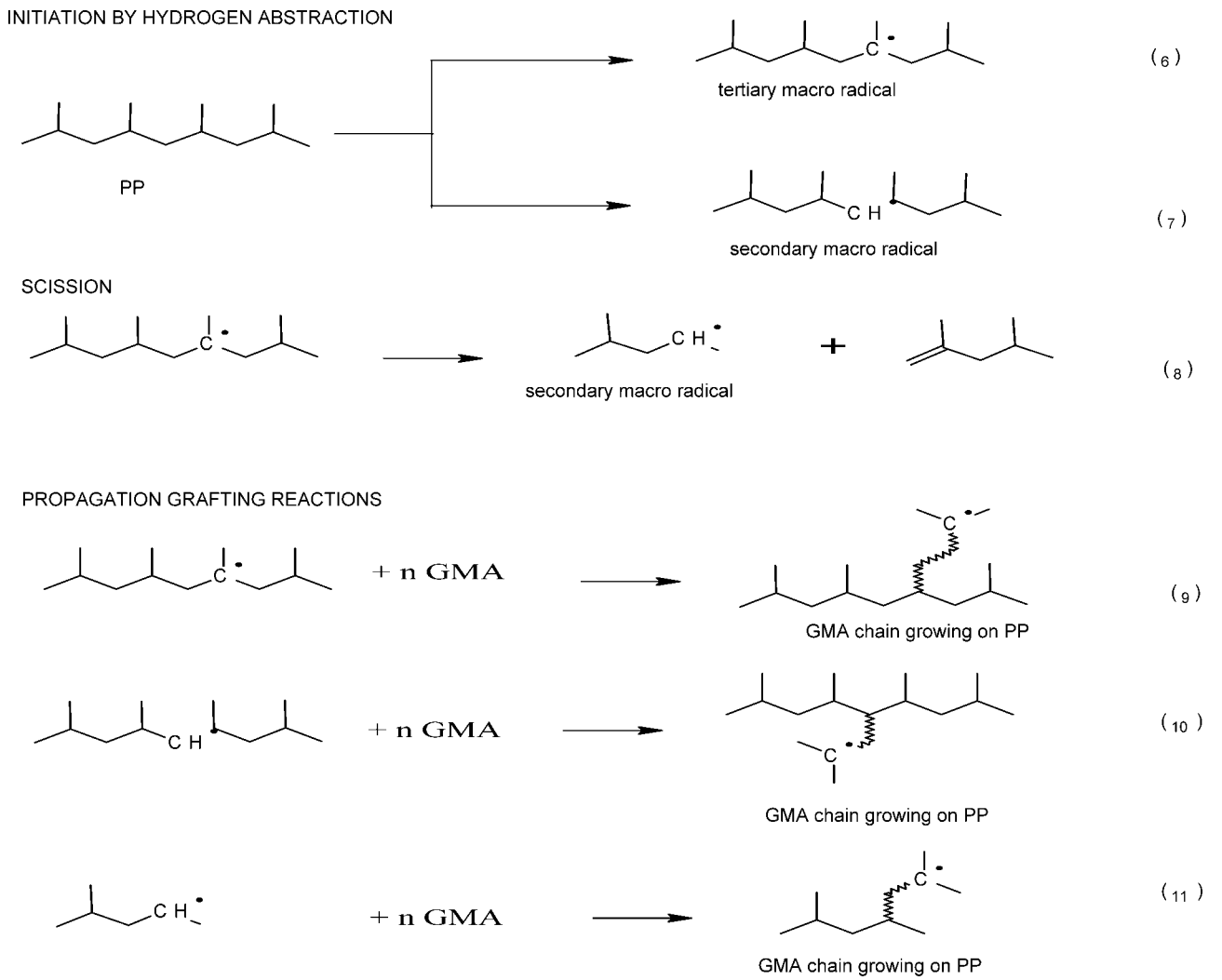

Scheme 1 Mechanism of grafting.

thickness of the BOPP films is shown in Figure 2. This stopping and range of ions in matter (SRIM) plot is based on results calculated with SRIM software. The 120-MeV Ag^{9+}-ion beam in PP has a 24.17-μm projected range. This is greater than the thickness of the BOPP film (15 μm) used, so an almost uniform energy deposition through the target is achieved. Moreover, its electronic energy loss value is 7.34 keV/nm; as a result, it has a high electronic LET. Thus, a considerable volume of BOPP around the ion projectile is influenced by the interaction between the Ag ions and the BOPP electrons. This results in the production of active chemical species such as cations, anions, electrons, and radicals along the ion path in the BOPP film. The Columbic attraction and repulsion among these active species cause violent bond stretching and segmental motion in the polymer chains, which lead to the distortion of PP's crystal lattice as well as bond breakage.[25] As a result of these bond cleavages, free hydrogen radicals and some other radicals are formed in the latent track. Subsequently, gaseous molecular species are formed by the combined mechanisms of the direct recombination of radicals and the recombination of diffusing radicals.[26] The bond breakages also lead to the formation of tertiary PP macroradicals, which, on spontaneous oxidation in air, generate hydroperoxide groups on PP. This is supported by the appearance of an OH band at 3400 cm^{-1} with a shoulder at 3555 cm^{-1} characteristic of hydroperoxide (OOH) groups[27] in the FTIR spectrum [Fig. 1(b)].

Because of the large variety of oxidation products in PP, the OOH band in the 3100–3800-cm^{-1} region and the carbonyl (C=O) bands in the 1500–1900-cm^{-1} region are less distinctly resolved. Moreover, the intensity of the band centered around 2900 cm^{-1} decreases [Fig. 1(c)] when BOPP is irradiated with Ag^{9+} (at $\Phi = 3 \times 10^{11}$ ions/cm^2). This can be attributed to the reduction in the molecular mass. Furthermore, the development of a yellow color and the creation of a new peak at 1642 cm^{-1} [Fig. 1(c)] confirm the formation of double bonds of dienes and trienes,

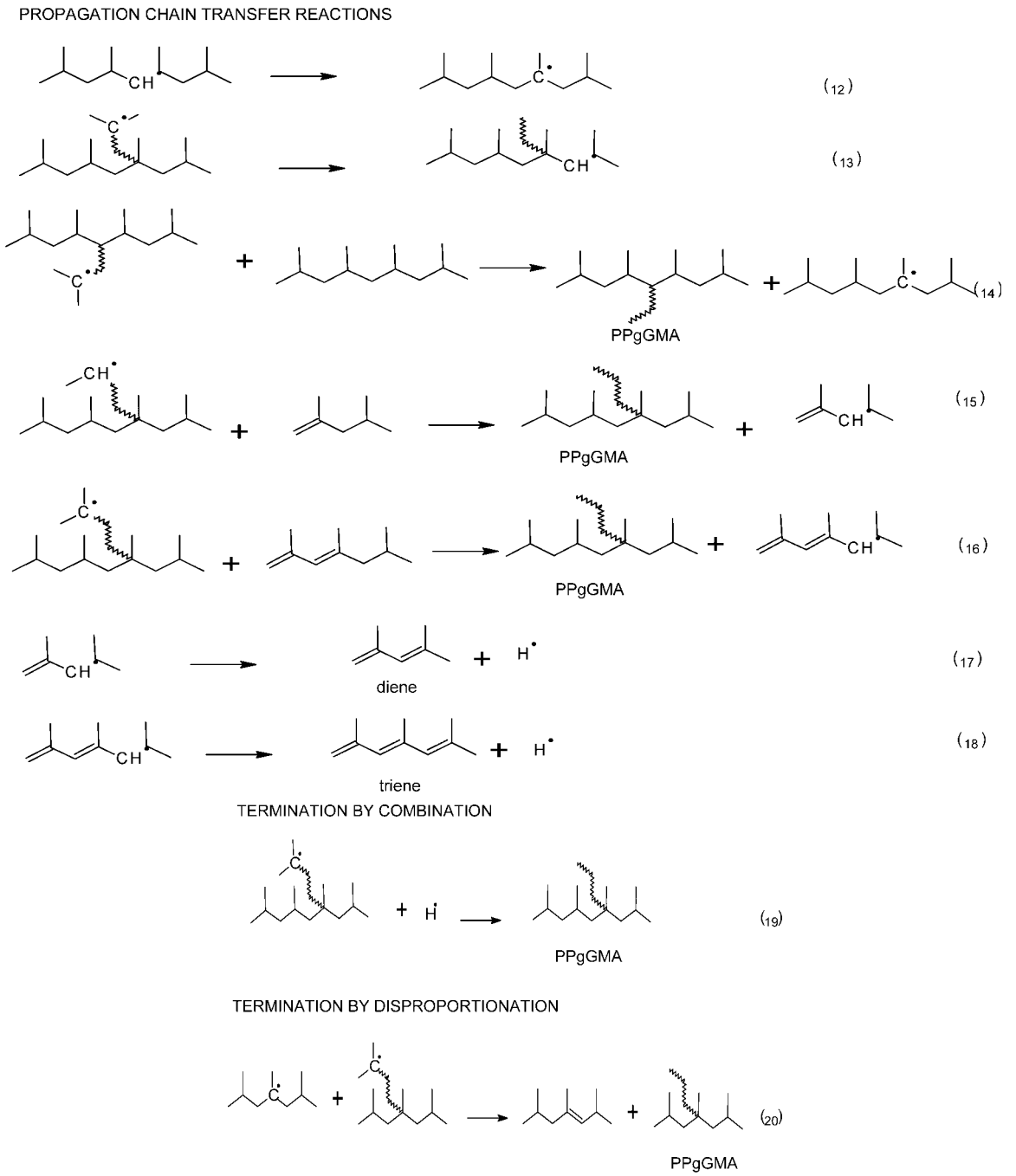

Scheme 1 (*Continued from the previous page*)

respectively, in the PP chains. The chain scissions and corresponding molecular weight reductions were minimized by the preferable use of the swift silver ions at fluencies not exceeding 3×10^{11} ions/cm^2. The same irradiation conditions also generated PP macroradicals and hydroperoxides needed for grafting on PP.[28] The FTIR spectrum of pure GMA is shown in Figure 1(d). It shows a C=O stretching peak at 1723 cm^{-1} due to the presence of a carbonyl group in GMA. It also shows a C=C stretching peak at 1639 cm^{-1} due to the presence of a vinyl unsaturation in GMA. Moreover, the absorptions at 908 and 844 cm^{-1} confirm the presence of the epoxide ring. The FTIR spectrum of a purified PP-*g*-GMA sample is shown in Figure 1(e). A comparison of the FTIR spectra [Fig. 1(d,e)] shows clearly the absence of absorption at 1639 cm^{-1} (C=C of GMA) in the grafted polymer, together with a redshift in the ester carbonyl absorption (a shift from 1723 to 1732 cm^{-1}), which is ascribed to the formation of a saturated ester. These results indicate that the grafting of GMA onto the BOPP film is clearly achieved. Addi-

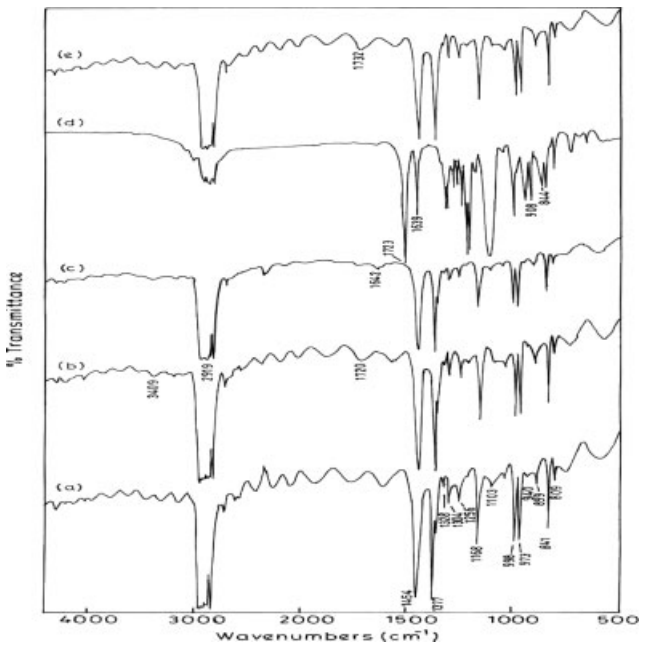

Figure 1 FTIR spectra of (a) unirradiated BOPP, (b) Ag^{9+}-irradiated BOPP ($\Phi = 3 \times 10^{10}$), (c) Ag^{9+}-irradiated BOPP ($\Phi = 3 \times 10^{11}$), (d) GMA, and (e) PP-*g*-GMA.

tionally, the intensity of this characteristic band at 1732 cm^{-1} increased with an increase in the graft level.

Morphological studies

The surfaces of the original BOPP, swift-silver-ion-irradiated BOPP, and GMA-grafted BOPP films were examined by SEM, and the results are shown in Figure 3.

The virgin BOPP film surface is flat along with abundantly distributed amorphous regions, which appear with a brighter intensity in the SEM photograph [Fig. 3(a)].[29]

The swift-silver-ion-irradiated BOPP film is composed of irradiated zones and unirradiated zones. The properties of BOPP remain unchanged in the unirradiated zones. However, the irradiated zones are highly modified zones of reduced density and reduced molecular weight, and they appear with a brighter intensity in the SEM photograph [Fig. 3(b)]. As the BOPP exhibits a crystalline structure, the diffusion of the GMA monomer is hindered in the unirradiated zones. However, the GMA monomer easily diffuses through the irradiated zones to encounter a reactive PP macroradical. The grafting is initiated as the reaction occurs between them. Subsequently, the grafted chains are able to grow by the polymerization of the GMA monomers coming from the outside of the film. A grafted macromolecule is generated in the track that can interpenetrate the PP chains when possible. Initially, with an increase in the fluence, the number of irradiated zones (and latent tracks and number of reactive sites) also increases. An increasing number of macroradicals propagate simultaneously; G_p increases, and the grafted chains grow to shorter lengths. As a result, only the spectrum of the graft is observed [Fig. 3(d)].

The absence of peaks or bands in the 3100–3800- and 1500–1900-cm^{-1} regions [Fig. 1(c)] of an irradiated BOPP sample at fluencies exceeding 10^{11} ions/cm^2 indicates that overlapping of the latent nuclear tracks occurs. This leads to an enhanced recombination of primary radicals before their reaction with the atmospheric oxygen can occur. When the latent tracks overlap, the number of initiating radicals decreases by termination reactions. Combination reactions result in the formation of crosslinked zones affecting the efficiency of grafting by hiding some radicals and/or modifying the diffusion rate of monomers.[17] Thus, a lower number of macroradicals are involved in propagation grafting reactions, so the length of the grafted chains gets bigger [Fig. 3(c)] and G_p decreases, even if the initial GMA concentration is kept constant. The obtained results are in agreement with the previously reported results.[30]

WAXD crystallographic studies

For isotactic PP, three crystalline forms, the monoclinic (α), hexagonal (β), and triclinic (γ) forms, have been reported on the basis of different X-ray diffraction patterns.[31] Of these three crystal structures, the α form is the most common and exists extensively in solution-crystallized or normal melt-crystallized samples. Only under rather stringent conditions can β and γ forms occur. The WAXD spectrum represents normalized diffraction intensities versus the diffraction angles (2θ). The monoclinic α crystal can be identified from WAXD measurements according to the

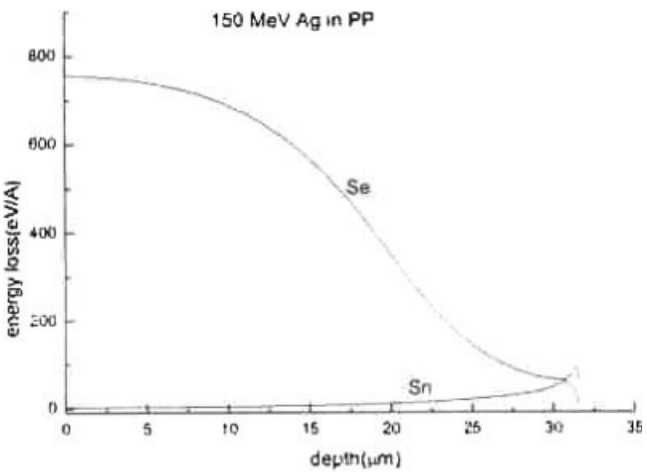

Figure 2 Variation of the electronic energy loss (S_e) and nuclear energy loss (S_n) of swift silver ions in PP across the thickness of the BOPP film: SRIM plot.

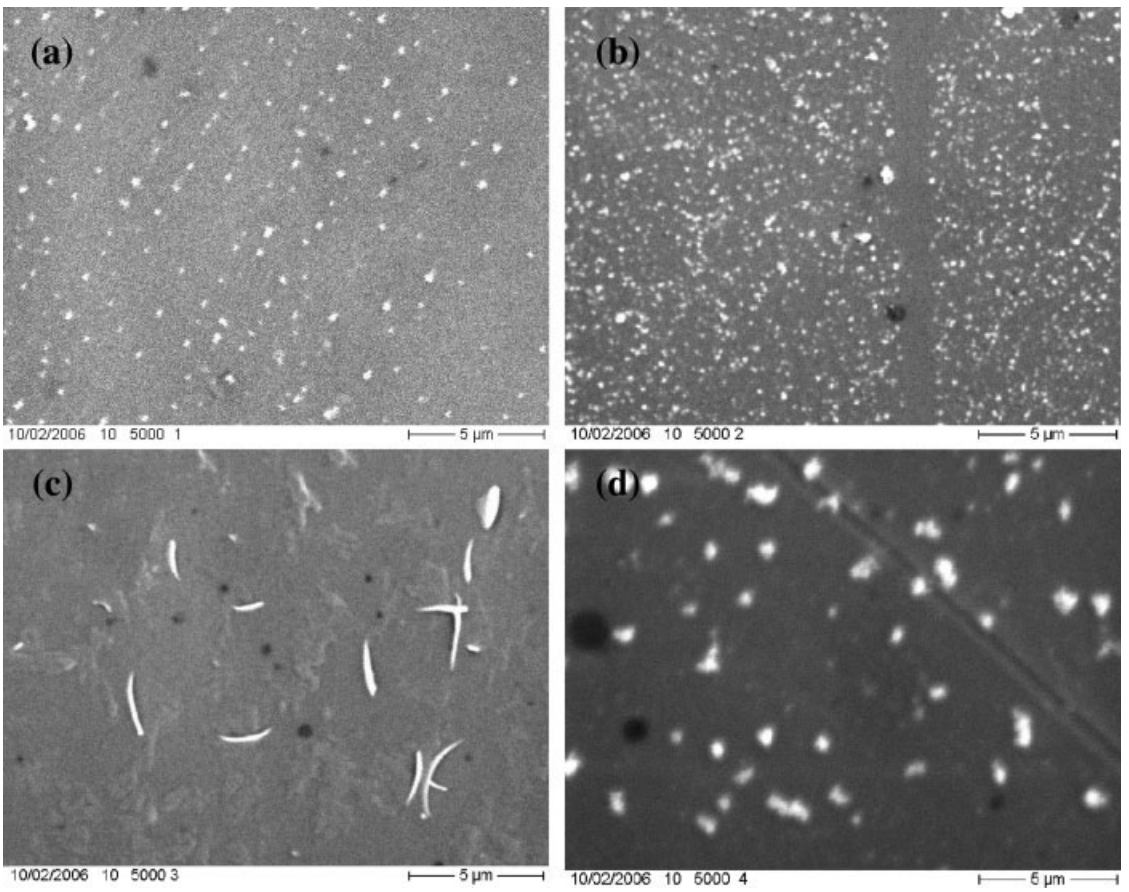

Figure 3 SEM photographs of (a) virgin BOPP, (b) Ag^{9+}-irradiated BOPP ($\Phi = 3 \times 10^{10}$), (c) Ag^{9+}-irradiated ($\Phi = 3 \times 10^{11}$) and GMA-grafted BOPP ($G_p = 5.26\%$), and (d) Ag^{9+}-irradiated ($\Phi = 3 \times 10^{10}$) and GMA-grafted BOPP ($G_p = 7.69\%$).

presence of diffraction peaks at 2θ values of 14.0 (110), 16.9 (040), 18.6 (130), 21.2 (111), and 21.9° (131), and the hexagonal β crystal can be identified at 16.1 (300), and 21.2° (301). Furthermore, the diagnostic diffraction peak of the γ crystal is at $2\theta = 20.1^\circ$ for crystal plane (117) because other diffraction peaks of the γ crystal overlap with the peaks of the α crystal.

Figure 4(a) presents a typical WAXD pattern of the virgin BOPP. It shows that the virgin BOPP film sample mainly consists of the α modification. Qualitative analysis shows that during the biaxial orientation of PP, there is displacement of the (130), (111), and (131) diffraction peaks. It can be attributed to a significant reorganization of molecules and, consequently, of crystalline regions in the process of biaxial solid-state drawing at an elevated temperature during the BOPP film production.[32] The WAXD curves of modified PP are shown in Figure 3(b–d). These WAXD patterns show that the PP-*g*-GMA samples mainly consist of the α modification. The obtained results are in agreement with the results previously reported by Pan et al.[11]

A strong peak appearing at $2\theta = 16^\circ$ indicates that the β crystals only exist in PP-*g*-GMA with 7.7 wt % grafting. The lack of a diffraction peak at $2\theta = 20.1^\circ$ implies that there is no γ crystal in the samples. The silver-ion-irradiation-induced GMA grafting causes important qualitative changes in the diffraction spec-

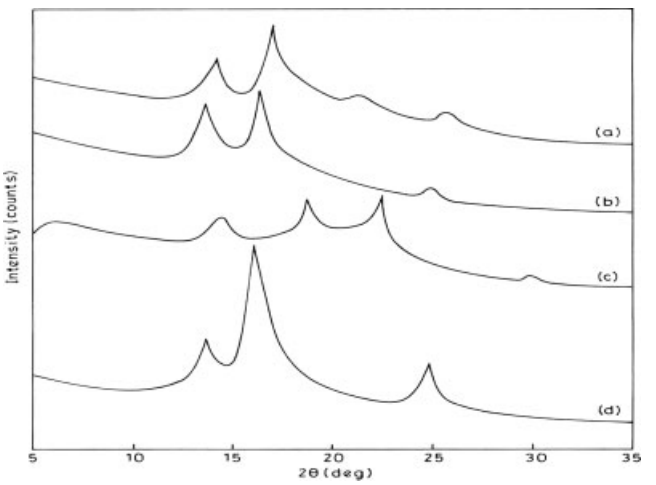

Figure 4 WAXD plots of (a) virgin BOPP, (b) Ag^{9+}-irradiated ($\Phi = 10^{10}$) and GMA-grafted BOPP ($G_p = 4.65\%$), (c) Ag^{9+}-irradiated ($\Phi = 3 \times 10^{10}$) and GMA-grafted BOPP ($G_p = 7.69\%$), and (d) Ag^{9+}-irradiated ($\Phi = 3 \times 10^{11}$) and GMA-grafted BOPP ($G_p = 5.26\%$).

TABLE I
fwhm (*b*) and Crystallite Size (*L*) of Virgin and PP-*g*-GMA Samples

Virgin BOPP			PP-*g*-GMA1			PP-*g*-GMA2			PP-*g*-GMA3		
2θ (°)	*b* (°)	*L* (Å)	2θ (°)	*b* (°)	*L* (Å)	2θ (°)	*b* (°)	*L* (Å)	2θ (°)	*b* (°)	*L* (Å)
12.18	0.10	888.5	13.67	0.96	92.7	13.64	0.20	445.1	6.08	0.96	92.2
14.18	0.80	111.3	16.40	0.40	223.3	16.06	0.28	318.6	14.49	0.96	92.8
17.00	0.40	223.3	24.91	0.48	188.5	24.89	0.48	188.5	18.84	0.80	111.9
25.44	0.96	94.34							22.60	0.32	281.4
									29.36	0.28	211.4

tra. An increase in the GMA grafting weight percentage either gives rise to new diffraction peaks or causes the disappearance of old ones. This means that silver-ion-induced GMA grafting on PP produces macromolecular reorganizations that are able to create new crystalline symmetries. Thus, the supermolecular structure and crystalline morphology of PP are affected by the grafting of GMA. We cannot deconvolute the amorphous, mesomorphic, and crystal phases with certainty because the WAXD profiles have a low signal-to-noise ratio. However, the identification of the polymorphic transitions α to β of PP can be clearly marked if we follow the occurrence of the peak at 16.0° (the β-phase 300 reflection). This polymorphic transition is unique and can be observed during the study of SHI-induced GMA grafting on BOPP.

The fwhm values and crystallite sizes of the virgin and PP-*g*-GMA samples are shown in Table I. The peaks for the PP-*g*-GMA1 and PP-*g*-GMA2 samples were shifted to smaller angles than that of the original BOPP. This clearly indicated that the interspacing of PP layers was swollen to a larger distance by the grafted GMA chains.[33]

Assuming $K = 1$ in the Scherrer equation, the average crystallite sizes of the virgin BOPP and GMA-grafted BOPP (PP-*g*-GMA) were calculated, and the results are shown in Table II. Pan et al.[11] reported that at a low level of GMA grafting on PP with a conventional solid-phase grafting method, large amounts of short graft chains acting as the nucleus agent speed up the crystallization process and therefore decrease the size of the crystal. However, at a high level of grafting, long graft chains hinder the crystallization, resulting in a large crystal particle. However, in this study, SHI-induced GMA grafting on BOPP indicated that the average crystallite size was dependent both on G_p and on the diene/triene content in the grafted samples.

UV–vis spectroscopy analysis

The appearance of new bands close to 240 and 290 nm in the UV spectrum (Fig. 5) confirms the formation of double bonds of dienes and trienes, respectively, in the PP chains.[34] Furthermore, in comparison with the PP-*g*-GMA1 sample, the PP-*g*-GMA2 sample had 111.4% more dienes and 191.3% more trienes. Apparently, some of these double bonds are in a cis configuration, which causes bending and twisting in the chains, so regular close packing becomes difficult. The polymer thus cannot crystallize readily and has a

TABLE II
Structure–Property Correlation in the Grafted Polymers

					Properties		
					Crystallization behavior		
No.	Sample	Fluency of 120-MeV Ag^{9+} ions (ions/cm^2)	G_p (wt %)	Structure	Crystalline form	Average crystallite size (Å)	Wetting property: contact angle (°)
1	Unirradiated BOPP	—	0.00	Isotactic, helical, nonpolar backbone	Monoclinic (α form)	329.4	53.0
2	PP-*g*-GMA1	1×10^{10}	4.65	Isotactic, helical, nonpolar backbone with small, polar polyGMA graft chains	Monoclinic (α form)	168.2	50.0
3	PP-*g*-GMA2	3×10^{10}	7.69	Isotactic, helical, nonpolar backbone with a large number of small, polar polyGMA graft chains	Hexagonal (β form)	317.4	48.0
4	PP-*g*-GMA3	3×10^{11}	5.26	Isotactic, helical, nonpolar backbone with a lower number of big, polar polyGMA graft chains	Monoclinic (α form)	157.9	48.5

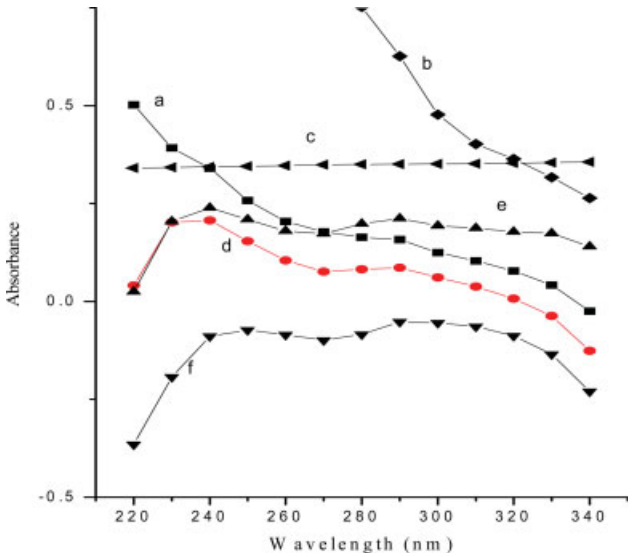

Figure 5 UV–vis absorption spectra of (a) Ag^{9+}-irradiated ($\Phi = 10^{10}$) BOPP, (b) Ag^{9+}-irradiated BOPP ($\Phi = 3 \times 10^{10}$), (c) Ag^{9+}-irradiated BOPP ($\Phi = 3 \times 10^{11}$), (d) Ag^{9+}-irradiated ($\Phi = 10^{10}$) and GMA-grafted BOPP ($G_p = 4.65\%$), (e) Ag^{9+}-irradiated ($\Phi = 3 \times 10^{10}$) and GMA-grafted BOPP ($G_p = 7.69\%$), and (f) Ag^{9+}-irradiated ($\Phi = 3 \times 10^{11}$) and GMA-grafted BOPP ($G_p = 5.26\%$). [Color figure can be viewed in the online issue, which is available at www.interscience.wiley.com.]

larger crystallite size. The average crystallite size was found to be directly dependent on the diene/triene content:

Diene/triene content : PP-*g*-GMA2 > PP-*g*-GMA1 > PP-*g*-GMA3

Average crystallite size : PP-*g*-GMA2 > PP-*g*-GMA1 > PP-*g*-GMA3

Studies of the wetting properties

The contact-angle results are shown in Table II. The contact-angle values of water droplets decreased with the grafting of GMA onto BOPP. This is because the PP-*g*-GMA samples were more hydrophilic and this property is dependent on the presence of GMA groups in them. The greater the grafting yield was, the less hydrophobic the PP-*g*-GMA samples were and, consequently, the greater the reduction was in the water contact angles.

CONCLUSIONS

This article concerns the development of a novel method for obtaining a grafted product. Using a commercial BOPP film, we grafted a GMA monomer, using swift Ag^{9+} ions. FTIR, UV–vis, WAXD, and contact-angle measurements show that there are significant modifications in the chemical structure, average crystallite sizes, and surface properties of PP upon swift-Ag^{9+}-ion-induced GMA grafting. It is concluded from a comparison of the FTIR spectra of virgin, irradiated, and grafted samples that GMA grafting occurs on PP. When the fluency increases, the evolution of the grafting yield can be explained in terms of overlapping of the latent tracks. From an analysis of the WAXD patterns, it has been observed that polymorphic transitions of α to β of PP occur at higher G_p values. Furthermore, the evolution of the average crystallite size when the grafting yield increases can be explained in terms of the effect of the length of graft chains as well as double and triple bonds on the crystallization process.

S. Chawla gratefully acknowledges the blessings of Dr. Ashok K. Chauhan, Founder President of Ritnand Balved Education Foundation (RBEF) and Amity Universe. He is also obliged to Prof. B. P. Singh, Senior Director of the Amity School of Engineering and Technology, and Prof. Anwar Ali, Head of the Department of Chemistry of Jamia Millia Islamia (India), for their guidance and encouragement. Thanks are also due to Prof. R. M. Mehra, Department of Electronics (South Campus) of Delhi University (India), and Prof. Harpal Singh, Head of the Centre of Biomedical Engineering of the Indian Institute of Technology at Delhi (India), who enabled the completion of part of this work.

References

1. Xu, G.; Lin, S. Macromol Sci Rev Macromol Chem Phys 1994, 34, 555.
2. Kim, M.; Kiyohara, S.; Satoshi, K.; Satoshi, T.; Saito, K.; Sugo, T. J Membr Sci 1996, 33, 117.
3. Nho, Y. C.; Park, J. S.; Jin, J. H. J Mater Sci Part A: Pure Appl Chem 1997, 34, 831.
4. Saito, K.; Kaga, T.; Yamagishi, H.; Furusaki, S. J Membr Sci 1989, 43, 131.
5. Choi, S. H.; Nho, Y. J Appl Polym Sci 1999, 71, 2227.
6. Zhu, J.; Deng, J.; Cheng, S.; Yang, W. Macromol Chem Phys 2006, 207, 75.
7. Liu, N. C.; Xie, H. Q.; Baker, W. E. Polymer 1993, 34, 4680.
8. Sun, Y. J.; Hu, G. H.; Lambla, M. Angew Makromol Chem 1995, 229, 1.
9. Sun, Y. J.; Hu, G. H.; Lambla, M. J Appl Polym Sci 1995, 57, 1043.
10. Pesetskii, S. S.; Makarenko, O. A. Russ J Appl Chem 2002, 75, 629.
11. Pan, Y.; Ruan, J.; Zhou, J. J Appl Polym Sci 1997, 65, 1905.
12. Rengarajan, R.; Vicic, M.; Lee, S. Polymer 1989, 30, 933.
13. Apel, P. Nucl Instrum Methods Part B 2003, 208, 11.
14. Betz, N.; Dapz, S. Guittet, M. J. Nucl Instrum Methods Part B 1997, 131, 252.
15. Shtanko, N, I.; Kabanov, V. Y.; Yoshida, M. Nucl Instrum Methods Part B 1999, 151, 416.
16. Porte-Durrieu, M, C.; Aymes-Chodur, C.; Betz, N. J Biomed Mater Res 2000, 52, 119.
17. Betz, N. Nucl Instrum Methods Part B 1995, 105, 55.
18. Mazzei, R.; Tadey, D.; Smolko, S.; Rocco, C. Nucl Instrum Methods Part B 2003, 208, 411.
19. Scherrer, P. Gott Nachar 1918, 2, 98.
20. Odian, G. Principles of Polymerization, 3rd ed.; Wiley: New York, 2004; p 718.

21. Huang, H.; Liu, N. C. J Appl Polym Sci 1998, 67, 1957.
22. Ratzsch, M.; Arnold, M.; Borsig, E.; Bucka, H.; Reichelt, N. Prog Polym Sci 2002, 27, 1195.
23. Zhu, X.; Yan, D.; Fang, Y. J Phys Chem B 2001, 105, 12461.
24. Parthasarthy, G.; Kannan, R. M. J Polym Sci Part B: Polym Phys 2002, 40, 2539.
25. Lee, E. H. Nucl Instrum Methods Part B 1999, 151, 29.
26. de Jong, M. P.; Maas, A. J. H.; Van Ijzendoom, L. J.; Klein, S. S.; de Voigt, M. J. A. J Appl Phys 1997, 82, 1058.
27. Raff, R. A. V. Crystalline Olefin Polymers; Interscience: New York, 1965; Part I, p 795.
28. Chawla, S.; Ghosh, A. K.; Ahmad, S.; Avasthi, D. K. Nucl Instrum Methods Part B 2006, 244, 248.
29. Aboulfaraj, M.; Ulrich, B.; Dahoun, A.; G'Sell, C. Polymer 1993, 34, 4817.
30. Betz, N.; Le Moel, A.; Duraud, J. P.; Balanzat, E. Macromolecules 1992, 25, 213.
31. Turner-Jones, A.; Aizlewood, J. M. Makromol Chem 1964, 75, 134.
32. Stojanovic, Z.; Kacarevic-Popovic, Z.; Galovic, S.; Milicevic, D.; Suljovrujic, E. Polym Degrad Stab 2005, 87, 279.
33. Li, J.; Zhou, C.; Gang, W. Polym Test 2003, 22, 217.
34. Apel, P. Y.; Didyk, A. Y.; Salina, A. G. Nucl Instrum Methods Part B 1996, 107, 276.